Modeling the Cell Biology of the Heat Shock Response of Barley Aleurone Cells

Rachael Heineman

December 11, 2012

Abstract

When heat shocked, plant cells distribute their energy to make a very different set of proteins than when at normal temperatures. Along with other secretory proteins, α-amylase is particularly affected by heat shock. This protein is responsible for digesting the starchy food stores contained in the endosperm of a barley seed. These starchy nutrients comprise the largest part of the food store that allows the seed to germinate. When barley is heat shocked, the cells$'$ production of α-amylase and other secretory proteins is largely reduced and a set of heat shock proteins that repair damaged proteins is produced. This change in protein synthesis is the result of selective destabilization of the mRNAs encoding α-amylase and other secretory proteins. In addition, the endoplasmic reticulum (ER) upon which these secretory protein mRNAs are translated into proteins undergoes major structural and compositional changes. The purpose of this project is to create and test a mathematical model to analyze how these elements interact to influence α-amylase production while the cell is under heat stress. Our current model and simulations are able to capture the impact of different temperature regimes and levels of fluidity on α-amylase synthesis and are in good qualitative agreement with the experimental data.

1 Motivation

My motivation for choosing this particular project stems from my participation in the Integrated Research in Biomathematics program this past summer. When the research term ended, our team had developed a preliminary model and system of differential equations. We had also been able to perform some numerical analysis using Matlab and obtained a rough solution of total concentrations of α-amylase. With more time, we wanted to be able to refine our model, introduce a new variable of membrane fluidity, and obtain a new solution that matched the literature more accurately. By combining this project with my senior project, I have been able to continue working on the project throughout the Fall 2012 semester and achieve many of our goals.

I find this project so interesting because of the practical applications that our research could have one day. Understanding how plants react to high temperature stress, and what the process of protein synthesis looks like under those conditions will be critical to address environmental changes imposed by climate change. This project has allowed me to experience one way that mathematics can play a crucial and practical role in solving the world's problems. It has also introduced me to biomathematics, which I am hoping to pursue in graduate school.

2 Introduction

We live in a world of constant climate change. Human beings have means of adjusting to changing temperatures. We can remove or add clothing, change location, or turn on our heat or air conditioning. Plants are not so fortunate. Once they have been placed in the ground, they must deal with the temperature conditions presented to them without mobility. One of the ways that plants can adapt to temperature extremes is to alter the proteins that they are producing [3]. During this paper, we will focus our studies on barley plants.

Under normal temperature conditions, a barley seed will intake water, triggering the release of gibberellic acid (GA) from the embryo into the aleurone layer. The aleurone layer houses the digestive proteins, including α-amylase, necessary to provide nutrients to the embryo. The insertion of GA triggers the release of these proteins into the endosperm, where all of the plants nutrients are stored. These proteins digest the nutrients and transform them into a form that the embryo can use as food. When the embryo receives these nutrients, it germinates and sends a shoot up out of the ground [3]. See Figure 1 for a diagram of the germination process.

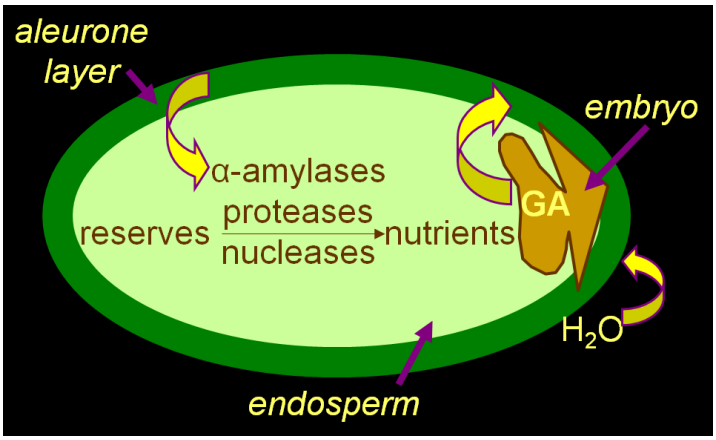

Figure 1: The process of germination for a barley seed [4].

When heat shocked, plant cells reallocate their energy to make different proteins than when at regular temperatures [3]. Along with other secretory proteins, α-amylase is particularly affected by heat shock. This protein is responsible for digesting the starchy food stores contained in the endosperm of a barley seed. These starchy nutrients comprise the largest part of the food store that allows the seed to germinate. When barley is heat shocked, the cells′ production of α-amylase and other secretory proteins is largely reduced and a set of heat shock proteins that repair damaged proteins is produced [16]. This change in protein synthesis is the result of selective destabilization of the mRNAs encoding α-amylase and other secretory proteins. In addition, the endoplasmic reticulum (ER) upon which these secretory protein mRNAs are translated into proteins undergoes major structural and compositional changes [2, 5].

The purpose of this project is to create a mathematical model to analyze how these elements interact to influence α-amylase production while barley aleurone cells are under heat stress. Our model was created using the mass-action principle to transform biological reactions into differential equations. We then fit the model with our experimental data which measure protein concentrations at three different temperature schemes (plunge, slow and fast ramps). The computational simulations show good qualitative agreement with the literature and experimental data. α-amylase is most severely affected by the plunge temperature scheme, but is not as drastically decreased in the slow ramp since the cells have enough time to adapt to the temperature stimulus [10].

Over the summer, we created the model and formed the original system of differential equations. We ran a preliminary analysis of the model, and compared the results to literature on the topic. This semester, we explored the concept of fluidity in the endoplasmic reticulum, and how it affects the synthesis of α-amylase. We gathered data on the two measurements of fluidity that we have, and created fitting functions for both types of data. We introduced these functions into our system of equations and reran our simulations. We also

normalized the data that we quantified over the summer in order to see if we could get the range of values to fall within the norms seen in literature reviews.

3 α-amylase Model Formation

We began our model formation by first obtaining an accurate schematic diagram of the process of α-amylase synthesis (see Figure 2). Then we assigned each reactant to a variable and used Figure 2 to write reaction equations for each step in the process.

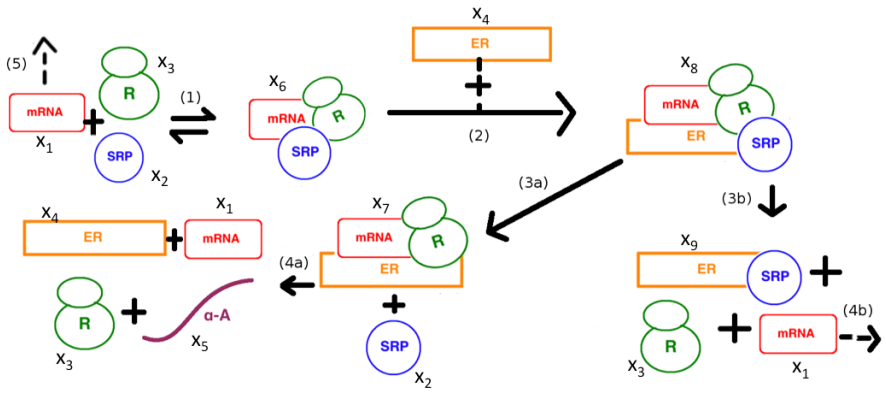

Figure 2: A schematic diagram illustrating the synthesis of α-amylase.

x_1 : α-amylase mRNA (mRNA)
x_2 : SRP
x_3 : Ribosomes (R)
x_4 : Endoplasmic Reticulum (ER)
x_5 : α-amylase (α-A)
x_6 : [mRNA $\cdot$ SRP $\cdot$ R]
x_7 : [ER $\cdot$ mRNA $\cdot$ R]
x_8 : [ER $\cdot$ mRNA $\cdot$ SRP $\cdot$ R]
x_9 : [ER $\cdot$ SRP]

Next we took each step of the synthesis reaction, translated the reactants into variables, and wrote reaction equations.

1. First, a signal recognition particle (SRP) joins with a ribosome and mRNA to form one complex.

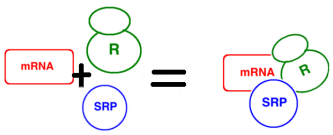

This first reaction is reversible and so is written as this reaction equation:

$$x_1 + x_2 + x_3 \underset{l_1}{\overset{k_1}{\rightleftarrows}} x_6.$$

2. Then the SRP transports this complex to the ER, where it attaches.

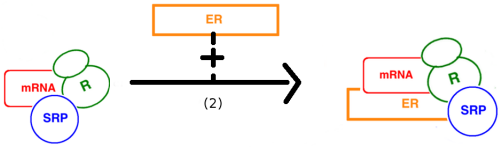

$$x_6 + x_4 \xrightarrow{k_2} x_8.$$

3. Next, the SRP disassociates, leaving the ribosome and mRNA attached to the ER.

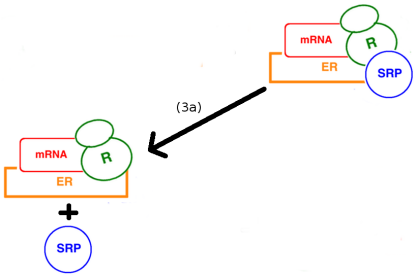

$$x_8 \xrightarrow{k_3} x_7 + x_2.$$

4. The signal tail of the α-amylase protein is inserted into the ER through a pore. The ribosome translates the rest of the mRNA strand into a full α-amylase protein. The mRNA and ribosome then disassociate and are free to begin the process again.

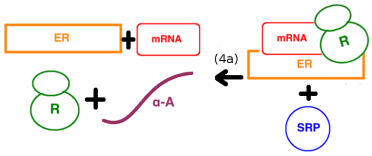

$$x_7 \xrightarrow{k_4} x_4 + x_1 + x_3 + x_5.$$

5. When heat shock occurs, there is a stall in the process of α-amylase synthesis. Steps 1 and 2 occur as normal, but instead of step 3, the SRP remains attached to the complex and the ER, and does not allow the ribosome to continue translation of the mRNA. The ribosome goes free, mRNA is degraded or detached, and the SRP remains stuck to the ER. No α-amylase protein is produced.

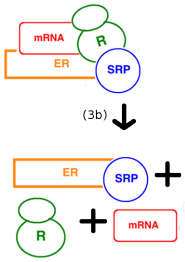

$$x_8 \xrightarrow{k_5} x_9 + x_3 + x_1.$$

6. While stuck on the ER, the mRNA is vulnerable to degradation by RNAses.

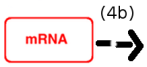

$$x_1 \xrightarrow{l_2} \text{degraded } x_1.$$

7. There is also a natural degradation process for mRNA. mRNa has a natural half life of 100 hours.

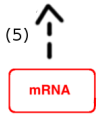

$$x_1 \xrightarrow{l_3} \text{degraded } x_1.$$

3.1 Mass-Action Law

In order to use these reaction equations to get a system of differential equations, we used the principle of mass action [14]. The principle of mass action states that the rate of each reaction is proportional to the concentration of reactants. Take the second reaction equation from above for example, $x_6 + x_4 \xrightarrow{k_2} x_8$. The concentrations of x_6 and x_4 are begin decreased at a rate of k_2, while the concentration of x_8 is being increased at the same rate. We write $\frac{dx_6}{dt} = \frac{dx_4}{dt} = -k_2 x_6(t) x_4(t)$, and $\frac{dx_8}{dt} = k_2 x_6(t) x_4(t)$. For a reversible reaction such as reaction one, $x_1 + x_2 + x_3 \overset{k_1}{\underset{l_1}{\rightleftarrows}} x_6$, we use a similar method. This time there are two rates to take into consideration. k_1 is the rate at which the concentrations of the reactants are changing with respect to the concentrations of x_1, x_2, and x_3 at time t. l_1 is the rate at which the concentrations of the reactants are changing with respect to the concentration of x_6 at time t. We obtain $\frac{dx_1}{dt} = \frac{dx_2}{dt} = \frac{dx_3}{dt} = -k_1 x_1(t) x_2(t) x_3(t) + l_1 x_6(t)$, and $\frac{dx_6}{dt} = k_1 x_1(t) x_2(t) x_3(t) - l_1 x_6(t)$. We perform this process for every rate equation and then sum all terms that contain each reactant to get a final differential equation for each reactant.

3.2 System of Differential Equations

The final differential equations for each reactant are detailed below. The first equation describes the rate of change for α-amylase mRNA. The rate of change of mRNA is influenced by the association and disassociation of the [mRNA·SRP·R] complex, the final production of the α-amylase protein, the disassociation of the elements after the synthesis stalls in step 5, the degradation of mRNA by RNAses, and the natural degradation of mRNA.

$$\frac{dx_1}{dt} = -k_1 x_1 x_2 x_3 + l_1 x_6 + k_4 x_7 + k_5 x_8 - l_2 x_1 - l_3 x_1.$$

The second equation describes the rate of change for SRP. The rate of change of SRP is influenced by the association and disassociation of the [mRNA·SRP·R] complex, and the expected disassociation of the SRP molecule during normal synthesis in step 3.

$$\frac{dx_2}{dt} = -k_1 x_1 x_2 x_3 + l_1 x_6 + k_3 x_8.$$

The third describes the rate of change for ribosomes. The rate of change of the concentration of ribosomes is influenced by the association and disassociation of the [mRNA·SRP·R] complex, the final production of the α-amylase protein, and the disassociation of the elements after the synthesis stalls in step 5.

$$\frac{dx_3}{dt} = -k_1 x_1 x_2 x_3 + l_1 x_6 + k_4 x_7 + k_5 x_8$$

The fourth describes the rate of change for the ER. The rate of change of the endoplasmic reticulum is influenced by the attachment of the [mRNA·SRP·R] complex to the ER, and the final production of the α-amylase protein.

$$\frac{dx_4}{dt} = -k_2 x_6 x_4 + k_4 x_7$$

The fifth describes the rate of change for α-amylase, which is influenced by the final production of the protein.

$$\frac{dx_5}{dt} = k_4 x_7$$

The sixth describes the rate of change for the [mRNA·SRP·R] complex. The rate of change for this complex is influenced by the association and disassociation of the [mRNA·SRP·R] complex, and the attachment of the [mRNA·SRP·R] complex to the ER.

$$\frac{dx_6}{dt} = -l_1 x_6 + k_1 x_1 x_2 x_3 - k_2 x_6 x_4$$

The seventh describes the rate of change for the [ER·mRNA·R] complex. The rate of change for this complex is influenced by the expected disassociation of the SRP molecule during normal synthesis in step 3, and the final production of the α-amylase protein.

$$\frac{dx_7}{dt} = k_3 x_8 - k_4 x_7$$

The eighth equation describes the rate of change for the [ER·mRNA·SRP·R] complex. The rate of change of this complex is influenced by the attachment of the [mRNA·SRP·R] complex to the ER, the expected disassociation of the SRP molecule during normal synthesis in step 3, the disassociation of the elements after the synthesis stalls in step 5, the changing temperature, denoted by the temperature function $F(T)$, and the change in the fluidity of the endoplasmic reticulum, denoted by $Fr(T)$ and $Ff(T)$. $Fr(T)$ accounts for the change in the ratio of fatty acids, and $Ff(T)$ accounts for the change in fluidity measured by fluorescence polarization. These quantities will be described in more detail in a later section. These functions for temperature and fluidity are included in the differential equation for [ER·mRNA·SRP·R] complex because temperature and fluidity influence whether step number 3 or step number 5 occur. This influences how large the terms in the eighth equation are.

$$\frac{dx_8}{dt} = k_2 x_6 x_4 - k_3 x_8 - k_5 x_8 + F(T) + Fr(T) + Ff(T)$$

Finally, the ninth describes the rate of change for the [ER·SRP] complex, which is influenced by the disassociation of the elements after the synthesis stalls in step 5.

$$\frac{dx_9}{dt} = k_5 x_8$$

3.3 Fourth-order Runge-Kutta method

Given a system of ordinary differential equations (ODEs), we can find a solution either numerically or analytically. When systems are large and complex, numerical methods must be used to obtain approximate solutions to the systems since the analytical techniques are not powerful enough.

The fourth-order Runge-Kutta method (RK4) is a 4-step numerical method used in Matlab ode45 to solve a system of ODEs. It is used because it provides a higher order of accuracy while balancing computation time.

We begin with an initial value problem: $\mathbf{y}' = \mathbf{f}(t, \mathbf{y})$, $\mathbf{y}(t_o) = \mathbf{y}_o$.

The RK4 method is:

$$\begin{aligned}
\mathbf{y}_{n+1} &= \mathbf{y}_n + \tfrac{1}{6}(\mathbf{k}_1 + 2\mathbf{k}_2 + 2\mathbf{k}_3 + \mathbf{k}_4), \\
t_{n+1} &= t_n + h, \\
\mathbf{k}_1 &= h\mathbf{f}(t_n, \mathbf{y}_n), \\
\mathbf{k}_2 &= h\mathbf{f}(t_n + \tfrac{1}{2}h, \mathbf{y}_n + \tfrac{1}{2}\mathbf{k}_1), \\
\mathbf{k}_3 &= h\mathbf{f}(t_n + \tfrac{1}{2}h, \mathbf{y}_n + \tfrac{1}{2}\mathbf{k}_2), \\
\mathbf{k}_4 &= h\mathbf{f}(t_n + h, \mathbf{y}_n + \mathbf{k}_3),
\end{aligned}$$

where h is the time step and $\mathbf{y}_{n+1}$ is an approximation of $\mathbf{y}(t_{n+1})$. The RK4 method has an error of order h^5 per step, and a total error of order h^4 [17].

3.3.1 Derivation

There is more than one way to derive the algorithm for RK4. I chose to follow the method of Jason Frank, a lecturer at the University of Amsterdam in the Netherlands [8]. His method requires understanding collocation methods, so I will present the explanation of how to use this method to approximate a solution to an ODE. Our goal is to find an approximation to the solution of

$$u'(t) = f(u(t)), \quad u(t_o) = y_o, \quad t \in [t_o, t_o + T]. \tag{1}$$

First we begin with some definitions that are necessary to understand this method.

Definition 1. *Ordinary differential equations (ODEs) are equations that involve a function and its derivatives.*

Definition 2. *A collocation method is a method used to numerically solve ordinary differential equations (ODEs), partial differential equations, and integral equations.*

Definition 3. *The interpolating polynomial $P(x) \in \mathbb{P}_{s-1}$ is the unique polynomial that satisfies $P(c_i) = g_i, i = 1, ..., s$, where c_i are the s distinct points and g_i are the corresponding data.*

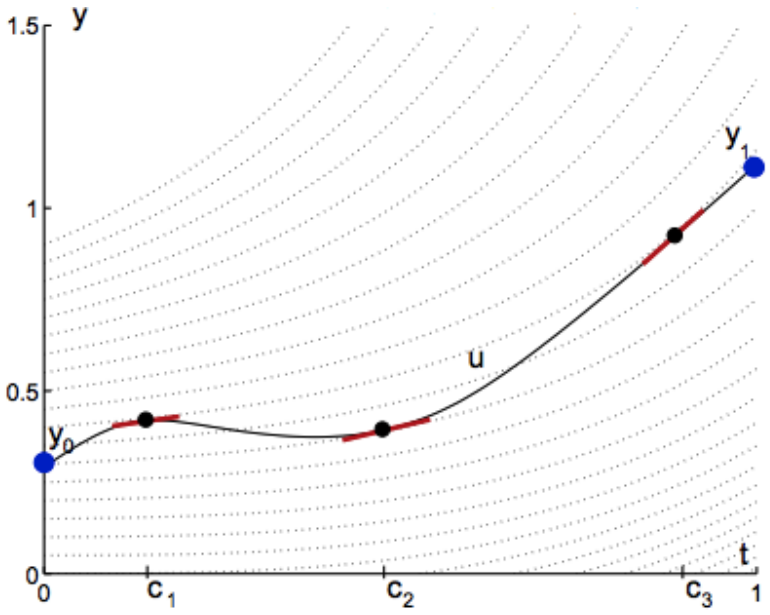

Figure 3: A collocation polynomial of degree three [12].

Definition 4. *The Lagrange interpolating polynomials* ℓ_i, $i = 1, ..., s$, *for a set of* s *points are defined by*

$$\ell_i(x) = \prod_{\substack{j=1 \\ j \neq i}}^{s} \left(\frac{x - c_j}{c_i - c_j}\right).$$

The interpolating polynomial for a function $g(x)$ is then given by $P(x) = \sum_{i=1}^{s} g_i \ell_i(x)$. We can then use the idea of collocation to construct a one-step method of given order of accuracy. We construct this method for the first time step interval $[t_o, t_o + h]$.

Let $0 \leq c_1 \leq c_2 \leq ... \leq c_s \leq 1$ be distinct nodes. The collocation polynomial $u(t) \in \mathbb{R}^d$ is a vector-valued polynomial of degree s satisfying the following:

$$\begin{aligned} u(t_o) &= y_o \\ u'(t_o + c_i h) &= f(u(t_o + c_i h)), \qquad i = 1, ..., s \end{aligned} \tag{2}$$

The numerical solution of the collocation method is given by $y_1 = u(t_o + h)$. In other words, we construct a polynomial that passes through y_o and matches equation (1) at s nodes on $[t_o, t_1]$. The numerical solution is then the value of this polynomial at time t_1. See Figure 3 for an example of such a polynomial. This method can be generalized to get the RK4 method using the following theorem.

Theorem 1. *The collocation method for $c_1, ..., c_s$ is equivalent to the s-stage Runge-Kutta method with coefficients*

$$a_{ij} = \int_0^{c_i} \ell_j(x)dx, \quad b_i = \int_0^1 \ell_i(x)dx, \quad i, j = 1, ..., s,$$

where $\ell_i(x)$ is the Lagrange polynomial. Moreover:

$$F_i = f(y_n + h\sum_{j=1}^{s} F_j a_{ij}),$$

$$y_{n+1} = y_n + h\sum_{j=1}^{s} F_j b_j, \quad i, j = 1, ...s.$$

Proof : Consider an ordinary differential equation u', such that $u'(t_o+c_ih) = f(u(t_o + c_ih))$, with initial condition $u(t_o) = y_o$, where the solution is $y_1 = u(t_o + h)$. Define F_i to be the unknown values of our interpolating polynomial at the s nodes. Then $F_i = u'(t_o + c_ih), i = 1, ..., s$. We emphasize that the values of F_i are the derivatives of the collocation polynomial, u. Now we use the formula for $P(x)$ that we defined earlier ($P(x) = \sum_{i=1}^{s} g_i\ell_i(x)$), along with a change of variable (let $t = t_o + xh$), to approximate $u'(t)$ with our interpolating polynomial. Then,

$$u'(t) = \sum_{i=1}^{s} F_i\ell_i\left(\frac{t - t_o}{h}\right). \tag{3}$$

Integrate over the interval from 0 to c_i (considering our variable change):

$$\int_{t_o}^{t_o+c_ih} u'(t)dt = h\int_0^{c_i}\sum_{j=1}^{s} F_j\ell_j(x)dx$$

$$\Rightarrow u(t_o + c_ih) - u(t_o) = h\sum_{j=1}^{s} F_j\int_0^{c_i}\ell_j(x)dx$$

$$\Rightarrow u(t_o + c_ih) = y_o + h\sum_{j=1}^{s} F_j a_{ij}.$$

Recall that $u'(t_o + c_ih) = f(u(t_o + c_ih))$. So,

$$u'(t_o + c_ih) = F_i = f(y_o + h\sum_{j=1}^{s} F_j a_{ij}), \quad i, j = 1, ..., s. \tag{4}$$

So, we have derived a useful formula for $u'(t_o+c_ih)$ by using the interpolating polynomial. Now, we also need to derive $y_1 = u(t_o + h)$. So we integrate

$u'(t_o + xh)$ over the interval $[0, 1]$:

$$\int_0^1 u'(t_o + xh)dx = h \int_0^1 \sum_{j=1}^{s} F_j \ell_j(x)dx$$

$\Rightarrow$

$$u(t_o + h) - u(t_o) = h \sum_{j=1}^{s} F_j \int_0^1 \ell_j(x)dx$$

$\Rightarrow$

$$u(t_o + h) = y_o + h \sum_{j=1}^{s} F_j b_j$$

So, $y_1 = u(t_o + h) = y_o + h \sum_{j=1}^{s} F_j b_j$ is our approximation of the solution to the ODE $u'(t_o + c_i h) = f(u(t_o + c_i h))$. We can now generalize these derivations to get a general form for y_n and y_{n+1}.

$\Rightarrow$

$$F_i = f(y_n + h \sum_{j=1}^{s} F_j a_{ij}),$$

and

$$y_{n+1} = y_n + h \sum_{j=1}^{s} F_j b_j, i, j = 1, ...s.$$

□

We can generalize this method to get the four-stage Runge-Kutta method by allowing $c_1 = 0$, $c_2 = \frac{1}{2}$, $c_3 = \frac{1}{2}$, and $c_4 = 1$. Then we introduce an alternative form of stage values Y_i, which can be defined as intermediate values of y at time $t_n + c_i h$. Let $Y_i = y_n + h \sum_{j=1}^{s} a_{ij} F_j$.

Definition 5. *Refer to Theorem 1 and define $F_j = f(Y_j)$. Then*

$$Y_i = y_n + h \sum_{j=1}^{s} a_{ij} f(Y_j), \qquad i = 1, ..., s,$$

$$y_{n+1} = y_n + h \sum_{i=1}^{s} b_i f(Y_i).$$

We can then write Runge-Kutta four as the following:

$$\begin{array}{lcl} Y_1 & = & y_n, \\ Y_2 & = & y_n + \frac{h}{2} f(Y_1), \\ Y_3 & = & y_n + \frac{h}{2} f(Y_2), \\ Y_4 & = & y_n + h f(Y_3), \\ y_{n+1} & = & y_n + h(\frac{1}{6} f(Y_1) + \frac{1}{3} f(Y_2) + \frac{1}{3} f(Y_3) + \frac{1}{6} f(Y_4). \end{array}$$

With a little bit of manipulation, we can see that this method of writing RK4 is equivalent to the method we began with at the start of this section. This method was understood based on lecture notes by Dr. Jason Frank [8].

4 Numerical Analysis

This section will describe the numerical analysis we performed on the system of nine differential equations presented earlier. We used MATLAB solver ode45, which uses the fourth-order Runge-Kutta method described previously, to perform our simulations.

4.1 Fitting Functions

First of all, we must define the $F(T)$, $Fr(T)$, and $Ff(T)$ functions that are present in the eighth differential equation. The $F(T)$ function makes it possible for us to include a temperature variable in our model. $F(T)$ describes how α-amylase synthesis responds to changes in temperature. For this project, we used data collected by Dr. Brodl and his students over the past twenty years. The data was recorded from barley aleurone layers treated in three types of temperature schemes [10].

We will call the first temperature scheme the plunge. During the plunge, barley aleurone layers were maintained in a 25°C water bath for three hours, and then plunged straight into a 40°C water bath. The barley aleurone layers were maintained at 40°C for three hours. Measurements were taken on the hour every hour, and every measurement recorded the amount of α-amylase produced in the previous half-hour.

The second temperature scheme will be called the fast ramp. During this scheme, barley aleurone layers also began in a 25°C water bath for three hours. The temperature of the water bath was then increased by 2.5°C every half hour until it reached 40°C. Measurements were taken at 0, 1, 2, 3, 4.5, 5, 5.5, and 6 hours, again measuring the amount of α-amylase produced in the previous half-hour.

We will call the final temperature scheme the slow ramp. During the slow ramp, barley aleurone layers once again began in a 25°C water bath. The temperature of the water bath was increased by 2.5°C every hour until it reached 40°C. Measurements were taken every hour on the hour for the last four hours of treatment. Figure 4 gives a good example of the fast and slow ramp time schemes. The six hours described above would go from 13 to 19 hours on this graph.

In order to get a function for $F(T)$, we had to fit one to the data that we compiled for α-amylase synthesis since there was no known temperature function for α-amylase. We began by using a simple third degree polynomial fit (see Figure 5).

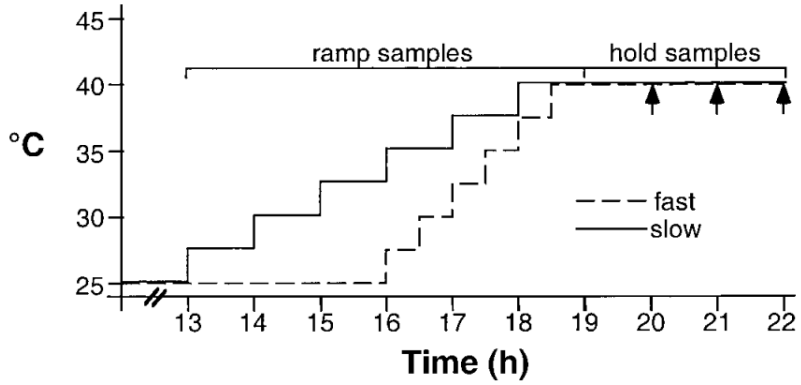

Figure 4: Example diagram of the fast and slow ramp time schemes [10].

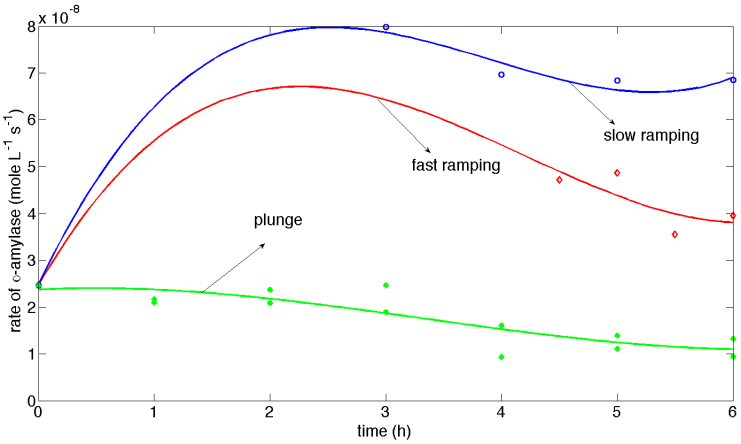

Figure 5: Original fitting functions for the three time schemes of α-amylase.

Because we are missing data for the first hours of the slow ramp time scheme, the polynomial fitting could create too much extrapolation for those first hours. We decided to use a piecewise linear fit instead, in order to get the most accurate function with the data that we had (see Figure 6).

4.2 Fluidity

$Fr(T)$, and $Ff(T)$ make it possible for us to include a fluidity variable in our model. How does fluidity influence synthesis of α-amylase? Fluidity refers to the fluidity of the endoplasmic reticulum (ER). The ER is composed of fatty acids that become more fluid when temperature is increased. This fluidity changes

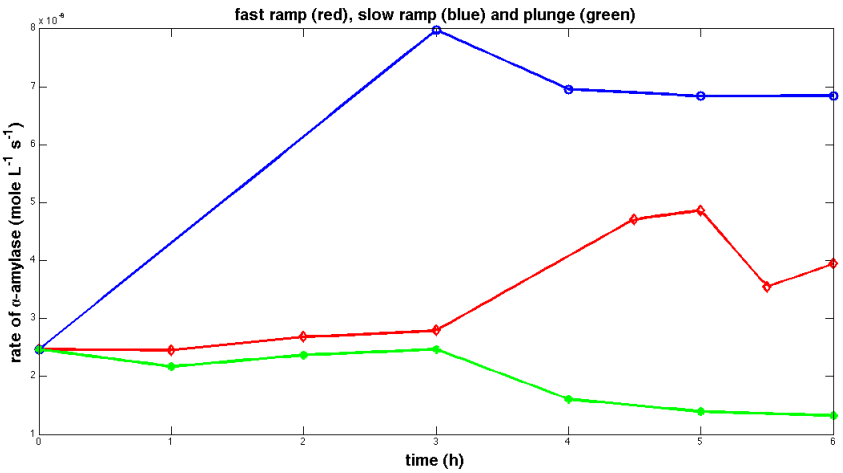

Figure 6: Revised fitting function for the three time schemes of α-amylase.

the structure of the ER and affects the functioning of a very important pore. During the process of α-amylase synthesis, the mRNA inserts its tail through a pore in the membrane into the ER, where the actual synthesis of α-amylase takes place. When the fluidity is altered, these pores cease to function properly and α-amylase cannot be produced inside of the ER. This stalls the synthesis process [9].

There are two measures of fluidity that we have data for: fatty acid ratios, and fluorescence polarization. Fatty acid ratios measure the ratio of saturated to unsaturated fatty acids in the endoplasmic reticulum. Fluorescence polarization measures the fluidity of the membrane by recording how much light is able to reflect back to the source. With each of these measurements, we only have data from the beginning and end points of our time intervals. Because of these limited data points, we had to use a strictly linear fitting approach where we associated the variable, fatty acid ratio or fluorescence polarization, with rates of α-amylase synthesis at those times. Below are the two fitting functions that we derived from this process for the plunge time scheme. Table 1 illustrates the data that we used in order to derive the functions. $Fr(T)$ describes the way that the rate of α-amylase synthesis changes with respect to the fatty acid ratio. $Ff(T)$ describes the way that the rate of α-amylase synthesis changes with respect to the fluorescence polarization data. See Figure 7 for a graphical representation of these functions.

Fluidity: Ff = (.173-.201)/(.1324-.2466)*(F-.2466)+.201;

Ratio: Fr = ((.88-.56)/(.1324-.2466)*(F-.2466)+.56;

Temperature (C)	Fluorescence	α-amylase	Ratio of fatty acids
25	.201	.2466	.56
40	.173	.1324	.88

Table 1: Fluidity data for the plunge time scheme.

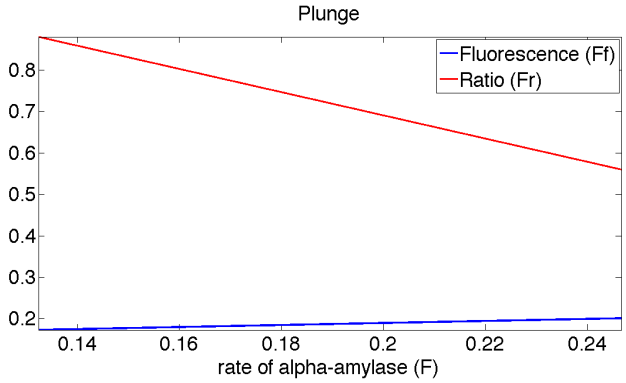

Figure 7: A graphical representation of Ff and Fr.

4.3 Parameters and Initial Values

We could not find reliable measurements of our parameters or steady state values of our reactants in the literature, so we made our best approximations of these values according to a range of sources[6, 15, 13, 1, 7, 11]. We obtained some values from literature, and we calculated some values based on relations and other known quantities. The results reported in the next section are based on the initial values of the variables (Table 2) and parameters (Table 3).

Variable	Description	Value ($\frac{mol}{L}$)
x_1	α-amylase mRNA	$8.7580 * 10^{-09}$
x_2	SRP	$2.2740 * 10^{-10}$
x_3	Ribosomes	$4.5495 * 10^{-08}$
x_4	Endoplasmic Reticulum	$3.8813 * 10^{-08}$
x_5	α-amylase	$5.8120 * 10^{-07}$
x_6	[mRNA $\cdot$ SRP $\cdot$ R]	$8.7580 * 10^{-11}$
x_7	[ER $\cdot$ mRNA $\cdot$ R]	$8.7580 * 10^{-11}$
x_8	[ER $\cdot$ mRNA $\cdot$ SRP $\cdot$ R]	$8.7580 * 10^{-12}$
x_9	[ER $\cdot$ SRP]	0

Table 2: Steady State Concentrations of Variables

Parameter	Description	Value
k_1	rate of ribosome binding to mRNA	$2.0790 * 10^{-09}$
k_2	rate of x_6 binding to ER	$3.3333 * 10^{-08}$
k_3	rate of successful SRP detachment from ER	$4.1579 * 10^{-07}$
k_4	rate of alpha amylase synthesis	$2.0790 * 10^{-07}$
k_5	rate of SRP remaining stuck to ER	$4.1579 * 10^{-09}$
l_1	rate of [mRNA $\cdot$ SRP $\cdot$ R] decomposition	$2.0790 * 10^{-12}$
l_2	rate of heat-shock induced mRNA degradation	$7.7017 * 10^{-04}$
l_3	rate of natural mRNA degradation	$1.9167 * 10^{-06}$

Table 3: Estimated model parameters; units for parameters are $(s)^{-1}(\frac{mol}{L})^{-n+1}$, where n is the number of variables in the term containing the parameter.

4.4 Simulation Results

Over the summer research term, we obtained preliminary results for our simulation. These results were promising in that the general trend of the total concentrations for α-amylase matched what we expected from the literature (see Figure 8). Johnston et al [10] documented in their experiments that slow ramp samples experienced little to no suppression of α-amylase production, while fast ramp samples fell below normal production for about an hour before recovering. These two samples were in stark contrast to the plunge samples, which took eighteen hours to recover to normal production. In our simulations, α-amylase was most severely affected by the plunge temperature scheme. In the slow ramp experiment, the barley aleurone layer cells had enough time to adapt so that amylase synthesis was not as drastically decreased. Finally, the fast ramp samples performed less normally than the slow ramp but much better than the plunge.

After we added the fluidity functions to our system of differential equations, we obtained the total concentrations found in Figures 9 and 10. The revised solutions to the system of ODEs gives us two more characteristics that lines up with our expectations. According to Dr. Mark Brodl, the total concentration for the fast ramp at 6 hours of simulation should be about 2/3 of the way up from the plunge to the slow ramp. In addition, the total concentration of α-amylase after six hours of the plunge time scheme should be about $0.005\frac{mol}{L^{-1}}$. As we can see in Figure 10, our final concentrations follow very closely to these trends.

5 Conclusion

In this paper, we have explained the process of α-amylase synthesis under normal and heat-shocked conditions. We have used the principle of mass action to transform a series of reaction equations into differential equations. We have

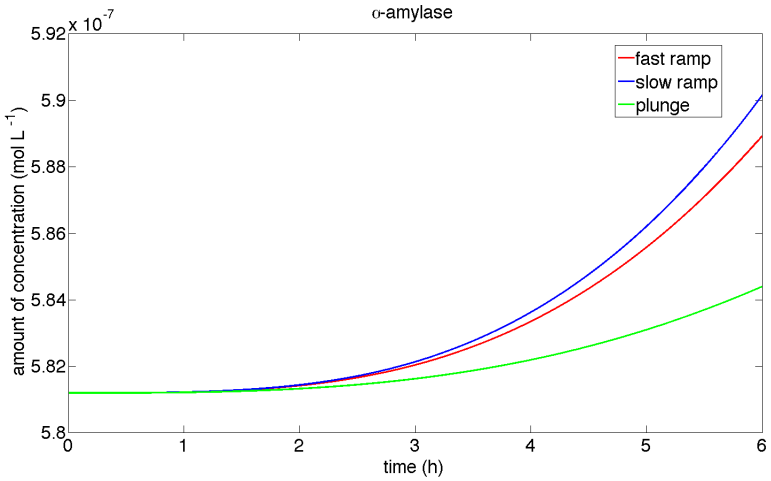

Figure 8: Total concentrations of α-amylase without fluidity.

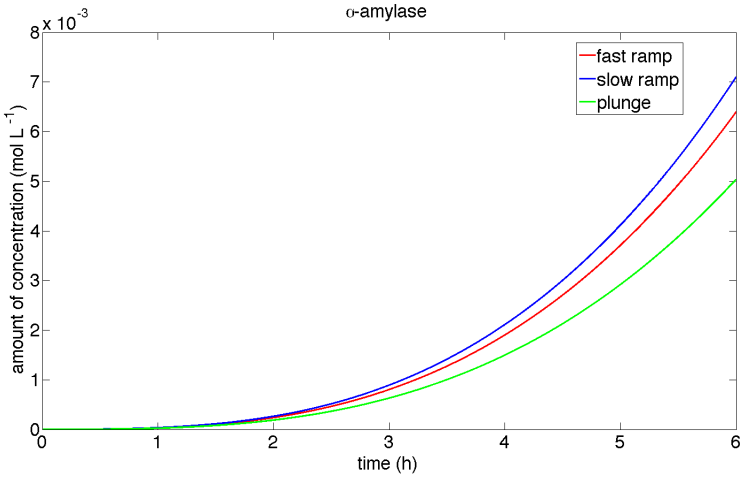

Figure 9: Revised total concentrations of α-amylase with fluidity data included.

derived a system of nine differential equations to model α-amylase synthesis, while taking into account both temperature and ER membrane fluidity.

We were able to achieve total concentrations with our simulations that have similar characteristics with information given by Dr. Brodl and with experimental data found in Johnston et al [10]. Future work on this project will be to continue to revise the system of differential equations to obtain simulation results that match even more closely with the expected behavior of α-amylase synthesis according to the literature. We would also like to compare our sim-

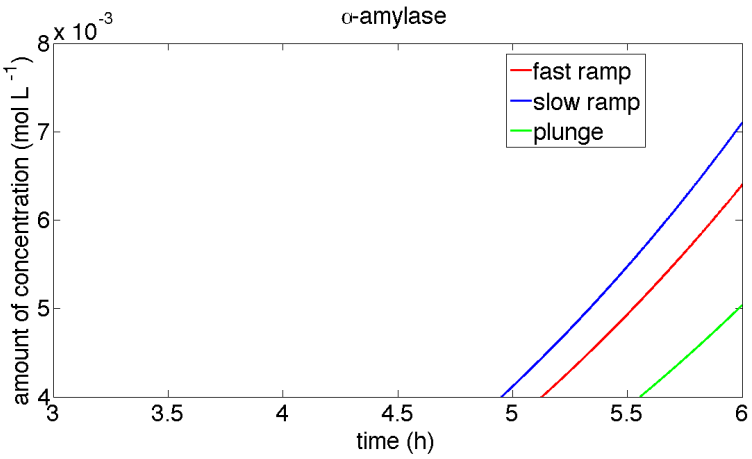

Figure 10: Zoom view of scale of final concentrations of α-amylase after six hours of simulation.

ulated plot for mRNA with data given to us by Dr. Mark Brodl in order to further validate our model. Once we have a more solid model, we would like to do sensitivity analysis to figure out which parameters are most sensitive to change.

6 Acknowledgements

I would like to thank Dr. Brodl and Dr. Nguyen for their assistance and participation in this project. It would not have been possible without them.

References

[1] Camara B., Hugueney P., Bouvier F., Kuntz M., and Monger R. Biochemistry and molecular biology of chromoplast development. *International Review of Cytology*, 163:175–247, 1995.

[2] Faith C. Belanger, Mark R. Brodl, and Tuan hua David Ho. Heat shock causes destabilization of specific mrnas and destruction of endoplasmic reticulum in barley aleurone cells. *Proc. Natl. Acad. Sci. USA*, 83:1354–1358, 1986.

[3] Mark R. Brodl. Regulation of the synthesis of normal cellular proteins during heat shock. *Physiologia Plantarum*, 75:439–443, 1989.

[4] Mark R. Brodl. Heat shock and unfolded protein responses in plant secretory cells, 2010.

[5] J. D. Campbell, L. A. Fielding, and M. R. Brodl. Heat shock temperature acclimation of normal secretory protein synthesis in barley aleurone cells. *Plant, Cell and Environment*, 20:1349–1360, 1997.

[6] Maarten J. Chrispeels and J.E. Varner. Gibberellic acid-enhanced synthesis and release of α-amylase and ribonuclease by isolated barley aleurone layers. *Plant Physiology*, 42:398–406, 1966.

[7] British Society for Cell Biology. Ribosome. `http://www.bscb.org/?url=softcell/ribo`.

[8] Jason Frank. Numerical modelling of dynamical systems: Chapters 7, 8. 2008.

[9] K. K. Grindstaff, L. A. Fielding, and M. R. Brodl. Effect of gibberellin and heat shock on the lipid composition of endoplasmic reticulum in barley aleurone layers. *Journal of Plant Physiology*, 1996.

[10] Mark K. Johnston, Paul A. S. Benson, Tracy M. Rodgers, and Mark R. Brodl. Slow heating of barley aleurone layers to heat-shock temperature preserves heat-shock-sensitive cellular properties. *American Journal of Botany*, 89:401–409, 2002.

[11] T. Krishnan and A. K. Chandra. Purification and characterization of ?-amylase from bacillus licheniformis cumc305. *Appl Environ Microbiol.*, 46:430–437, 1983.

[12] Florian Landis. Runge-kutta and collocation methods. 2005.

[13] Thomas J. Mozer. Partial purification and characterization of the mrna for α-amylase from barley aleurone layers. *Plant Physiology*, 65:834–837, 1980.

[14] Ion Petre, Andrzej Mizera, Claire Hyder, Andrey Mikhailov, John Eriksson, Lea Sistonen, and Ralph-Johan Back. A new mathematical model for the heat shock response, 2008.

[15] Nadav Skjøndal-Bar and David R. Morris. Dynamic model of the process of protein synthesis in eukaryotic cells. *Bulletin of Mathematical Biology*, 69:361–393, 2007.

[16] Zuzanna Szymanska and Maciej Zylicz. Mathematical modeling of heat shock protein synthesis in response to temperature change. *Journal of Theoretical Biology*, 2009.

[17] Runge-kutta methods. `http://en.wikipedia.org/wiki/Runge-Kutta_methods`.